Proteolytic targeting of Rab29 by an effector protein distinguishes the intracellular compartments of human-adapted and broad-host *Salmonella*

Stefania Spanò, Xiaoyun Liu, and Jorge E. Galán[1]

Section of Microbial Pathogenesis, Yale University School of Medicine, New Haven, CT 06536

Edited by Scott J. Hultgren, Washington University School of Medicine, St. Louis, MO, and approved October 5, 2011 (received for review July 21, 2011)

Unlike broad-host *Salmonella* serovars, which cause self-limiting disease, *Salmonella enterica* serovar Typhi can infect only humans causing typhoid fever, a life-threatening systemic disease. The molecular bases for these differences are presently unknown. Here we show that the GTPase Rab29 (Rab7L1) distinguishes the intracellular vacuole of human-adapted and broad-host *Salmonella* serovars. A screen to identify host factors required for the export of typhoid toxin, which is exclusively encoded by the human-specific *Salmonella enterica* serovars Typhi (*S.* Typhi) and Paratyphi (*S.* Paratyphi) identified Rab29. We found that Rab29 is recruited to the *S.* Typhi-containing vacuole but not to vacuoles containing broad-host *Salmonella*. We observed that in cells infected with broad-host *Salmonella* Rab29 is specifically cleaved by the proteolytic activity of GtgE, a unique type III secretion effector protein that is absent from *S.* Typhi. An *S.* Typhi strain engineered to express GtgE and therefore able to cleave Rab29 exhibited increased intracellular replication in human macrophages. These findings indicate significant differences in the intracellular biology of human-adapted and broad-host *Salmonella* and show how subtle differences in the assortment of effector proteins encoded by highly related pathogens can have a major impact in their biology.

bacterial pathogenesis | vesicular traffic | cysteine proteases

An intracellular pathogen, *Salmonella enterica* serovar Typhi (*S.* Typhi) causes typhoid fever and is a serious global health concern that results in >200,000 annual deaths, mostly in developing countries (1, 2). *S.* Typhi and the related serovar *Salmonella* Paratyphi can infect only humans, resulting in life-threatening systemic disease (i.e., "typhoid fever"). In addition, *S.* Typhi can cause life-long persistent infection in convalescent individuals (3). These features are in sharp contrast to most other *S. enterica* serovars such as *Salmonella* Typhimurium (*S.* Typhimurium) and *Salmonella* Enteritidis (*S.* Enteritidis). which can infect a variety of hosts and are usually associated with self-limiting gastroenteritis (i.e., "food poisoning") (4). The molecular bases for *S.* Typhi's unique pathogenic attributes are unknown although they are believed to be the result of a combination of genome degradation and the acquisition of new genetic information (5). It is also unknown whether the genetic differences between human-adapted and broad-host range *Salmonellae* may result in specific differences in the intracellular biology of these pathogens.

One of the few unique virulence factors of the human-adapted *S. enterica* serovars Typhi and Paratyphi is typhoid toxin (6–8), an AB toxin with DNase and ADP-ribosyl transferase activities. A distinguishing feature of this toxin is that it is produced only once *S.* Typhi reaches an intracellular location (7), and it is subsequently transported to the extracellular environment by a unique transport mechanism that involves vesicular transport intermediates (6). In an attempt to identify potentially unique properties of *S.* Typhi's intracellular biology, we sought to identify host cell factors that are necessary for the formation of the typhoid toxin transport intermediates. We show here that one of these factors, the Rab GTPase Rab29, is recruited to the *S.* Typhi-containing vacuole but not to the vacuole containing broad-host *Salmonella* serovars. We found that absence of recruitment of Rab29 to broad-host *Salmonella*-containing vacuoles is due to the specific cleavage of this GTPase by a unique type III secretion effector protein, which is absent in *S.* Typhi and *S.* Paratyphi. These results demonstrate that there are significant differences between the intracellular biology of human-adapted and broad-host range *S. enterica* serovars that could help explain differences in their pathogenic properties. In addition, our results showed that small differences in the battery of effectors delivered by virtually identical type III secretion systems can result in marked differences in the biology of highly related pathogens.

Results

Identification of Rab GTPases involved in the formation of typhoid toxin transport intermediates. We have previously shown that typhoid toxin is produced exclusively within host cells and that it is then transported to the extracellular environment by vesicular transport intermediates that can be visualized as puncta following immunofluorescence staining of the toxin (6). We sought to identify host cell factors necessary for the formation of these transport intermediates as a strategy to potentially identify unique features of the intracellular biology of *S.* Typhi. We specifically focused on Rab-family GTPases given their demonstrated role in vesicle trafficking (9, 10). We performed a siRNA screen targeting each of the human Rab and Rab-like GTPases (*SI Appendix*, Table S1) and found that depletion of Rab7, Rab29 (also known as Rab7L1), and Rab40B resulted in a significant reduction of the amount of typhoid toxin transport intermediates (Fig. 1 *A* and *B* and *SI Appendix*, Fig. S1). Most likely, this reduction is not due to reduced bacterial entry because the levels of bacterial internalization in cells depleted of Rab7, Rab29, or Rab40B were equivalent to those of control cells (Fig. 1*C*). However, depletion of Rab7 resulted in a marked decrease in the levels of *S.* Typhi intracellular replication (Fig. 1*D*), consistent with the previous observation that this GTPase is required for proper intracellular trafficking of *S.* Typhimurium (11). Therefore, the decrease of intracellular typhoid toxin puncta in cells depleted of Rab7 may be due to the reduced number of intracellular bacteria. In contrast, depletion of Rab29 or Rab40B in epithelial cells did not alter the levels of *S.* Typhi intracellular replication (Fig. 1*D*) or the levels of toxin production (*SI Appendix*, Fig. S1), suggesting a more specific role for Rab29 and Rab40B in toxin transport. Very little information is available on Rab29 and Rab40B. Rab29 is related to Rab32 and Rab38 (*SI Appendix*, Fig. S2), which are involved in the transport of melanocytic enzymes from the Golgi apparatus to the melanosomes (12). Rab40B, along with its close homologs Rab40A and Rab40C, forms an independent subgroup of Rab

Author contributions: S.S. and J.E.G. designed research; S.S. and X.L. performed research; S.S., X.L., and J.E.G. analyzed data; and S.S., X.L., and J.E.G. wrote the paper.

The authors declare no conflict of interest.

This article is a PNAS Direct Submission.

[1]To whom correspondence should be addressed. E-mail: jorge.galan@yale.edu.

This article contains supporting information online at www.pnas.org/lookup/suppl/doi:10.1073/pnas.1111959108/-/DCSupplemental.

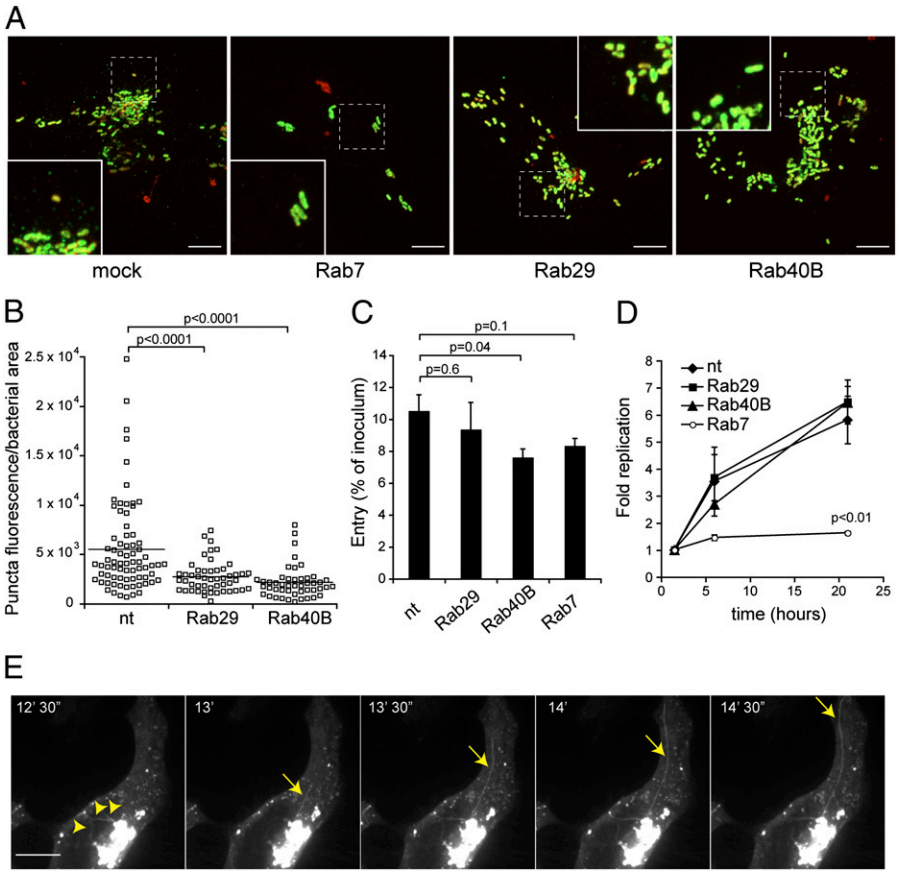

Fig. 1. Rab29 and Rab40B are required for the formation of typhoid toxin transport intermediates. (*A*) HeLa cells were transfected with siRNAs targeting the indicated human Rab and Rab-like GTPase proteins, infected with *S.* Typhi expressing 3×FLAG-tagged CdtB, and stained with anti-FLAG (green) and anti-*S.* Typhi (red) antibodies. Shown are maximum intensity projections of confocal Z-scans of cells mock treated or treated with siRNAs directed to the indicated Rab GTPases. *Insets* show enlargement of the dashed area to highlight toxin transport intermediates. (Scale bars, 10 μm.) (*B*) Quantification of typhoid toxin-containing puncta in Henle-407 cells transfected with siRNAs targeting Rab29 or Rab40B or with a nontargeting (nt) siRNA smart pool. Squares represent values for 60×-magnification images from two independent experiments and bars represent the means. Student's *t* test analysis was performed and the *P* values are shown. (*C* and *D*) Levels of *S.* Typhi internalization (*C*) and replication (*D*) within cultured Henle-407 cells transfected with siRNAs targeting Rab29, Rab40B, or Rab7 or with a nontargeting (nt) siRNA smart pool. Values of bacterial colony-forming units (CFU) are the means ± SEM of at least three independent determinations. *P* values were determined by Student's *t* test. (*E*) Time-lapse video microscopy sequence of Henle-407 cells expressing GFP-Rab29. Maximum intensity projections of confocal Z-scans from selected time frames are shown. Arrowheads and arrows indicate short tubular and long tubular structures, respectively, emanating from the Golgi (entire sequence in Movie S1). (Scale bar, 10 μm.)

GTPases (*SI Appendix*, Fig. S2). We found that Rab29 colocalizes with the Golgi marker GM130 (*SI Appendix*, Fig. S3). Live imaging showed that Rab29 localizes not only to the Golgi complex, but also along lengthy and dynamic tubules emerging from and retracting to the Golgi complex (Fig. 1*E*) (Movie S1). In contrast, Rab40B was found enriched at the nuclear envelope and in some punctate structures in the perinuclear area (*SI Appendix*, Fig. S3).

Rab29 is recruited to the *S.* Typhi-containing vacuole but not to vacuoles containing broad-host *S. enterica* serovars. We examined the localization of Rab40B and Rab29 in cultured cells infected with *S.* Typhi. We found that Rab40B was not recruited to the *S.* Typhi-containing vacuole and that its overall distribution throughout the cell was not altered by the bacterial infection (*SI Appendix*, Fig. S4). These observations suggest that this GTPase may affect the formation of toxin carriers indirectly and not by acting on the bacteria-containing vacuole. In contrast, Rab29 was efficiently recruited to the *S.* Typhi-containing vacuole ~90–120 min after bacterial internalization, with maximum recruitment ~3 h after infection (Fig. 2 *A* and *B*, *SI Appendix*, Fig. S5, and Movies S2 and S3), and remained associated with the bacteria-containing vacuole for several hours postrecruitment (Fig. 2*B*). Time-lapse video microscopy also showed highly dynamic tubules containing Rab29 connecting the Golgi apparatus and the bacterial vacuole as well as emerging from the vacuole toward the cell periphery (Fig. 2*C* and Movies S3 and S4). Recruitment of Rab29 to the *S.* Typhi vacuole was also observed in macrophages (*SI Appendix*, Fig. S6). The localization of Rab29 to the vacuole coincided with the time frame in which typhoid toxin puncta are observed after bacterial infection (6).

We then examined whether there were differences between the recruitment of Rab29 to the *S.* Typhi and the *S.* Typhimurium-containing vacuoles. In sharp contrast with *S.* Typhi, we found that Rab29 was not detected in *S.* Typhimurium vacuoles in epithelial cells (Fig. 2 *B* and *D* and *SI Appendix*, Fig. S5) or macrophages (*SI Appendix*, Fig. S6). These observations were not due to peculiarities of the specific isolates used in this study because we found similar phenotypes in several isolates of *S.* Typhi and *S.* Typhimurium (*SI Appendix*, Fig. S7). We also found efficient recruitment of Rab29 to the human-adapted serovar *S.* Paratyphi vacuoles but not to the vacuoles containing the broad-host range *S.* Enteritidis or *Salmonella* Dublin serovars (Fig. 2*E*). These findings are remarkable because this is a unique report of a host cell determinant that distinguishes the intracellular compartments containing human-adapted *S. enterica* serovars (i.e., *S.* Typhi and *S.* Paratyphi) from those containing broad-host range serovars (e.g., *S.* Typhimurium and *S.* Enteritidis). Furthermore, given the central role of Rab-family GTPases in vesicle trafficking (9, 10), it is expected that the presence or absence of Rab29 must translate into significant differences in the composition and properties of the bacteria-containing vacuoles.

Differential recruitment of Rab29 to the *S.* Typhi- and *S.* Typhimurium-containing vacuoles is dependent on the SPI-1 T3SS effector protein GtgE. We further investigated the basis for the observed differences in the recruitment of Rab29 among *S. enterica* serovars. Because the interaction of all *S. enterica* serovars with host cells is largely mediated by type III secretion systems (T3SSs) encoded within its pathogenicity islands 1 (SPI-1) and 2 (SPI-2) (13–15), we investigated the potential involvement of these systems in the recruitment of Rab29. However, we found that mutants defective in these systems were fully competent in the recruitment of Rab29 to the *S.* Typhi-containing vacuole (*SI Appendix*, Fig. S8). We therefore explored the possibility that *S.* Typhimurium may encode a factor (missing from *S.* Typhi) that would actively prevent the recruitment of Rab29 to its vacuole. To test this hypothesis, we

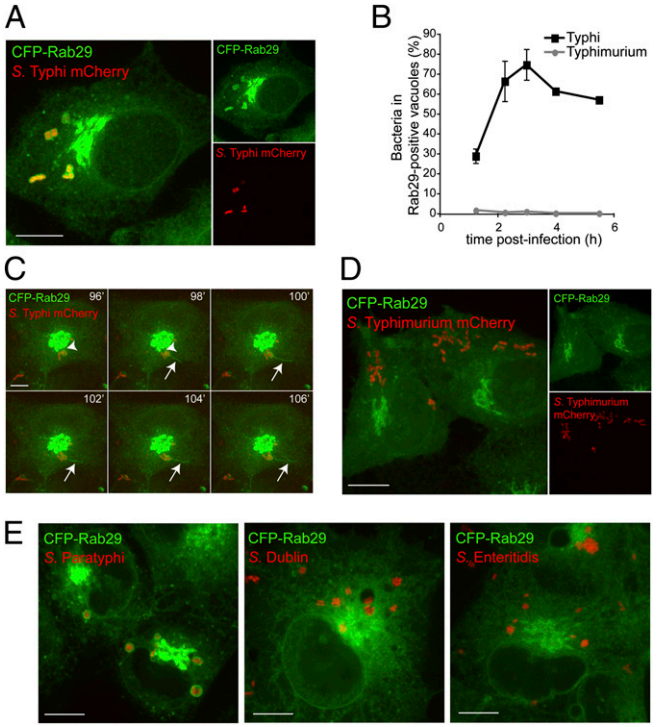

Fig. 2. Recruitment of Rab29 to *Salmonella*-containing vacuoles. Henle-407 (*A* and *D*) or COS-1 (*B*, *C*, and *E*) cells expressing CFP-Rab29 (green) were infected with *S.* Typhi (*A*–*D*), *S.* Typhimurium (*B* and *D*), or the indicated *S. enterica* serovars (*E*) expressing plasmid-borne fluorescent protein mCherry (red) for 1 h and treated with 100 μg/mL gentamicin for 1 h. In *A*, *D*, and *E* cells were imaged 3 h after the addition of bacteria. The images represent maximum-intensity projections of Z-stacks. (Scale bars, 10 μm.) In *B*, cell images were acquired at the indicated time points and the quantification of bacteria in Rab29-positive vacuoles at the times indicated is shown. Data are means ± SEM of three independent experiments in which at least 100 bacteria were counted for each time point. *C* shows a time-lapse video microscopy sequence starting 90 min postinfection. Maximum-intensity projections of confocal Z-scans from selected frames are shown. Tubular structures connecting the *Salmonella* connecting with the Golgi (arrowheads) or going into the cell periphery (arrows) are indicated (entire sequence in Movie S4).

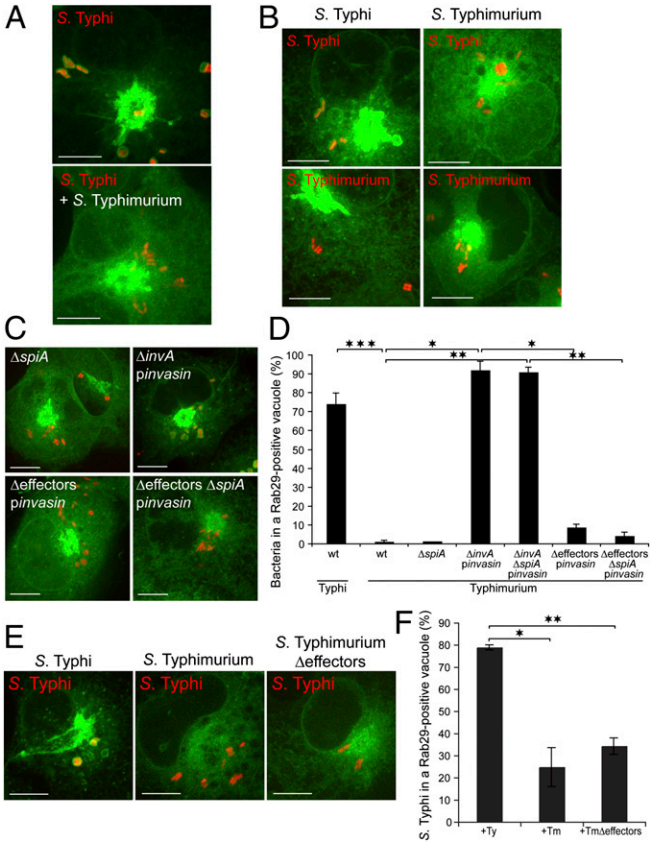

Fig. 3. The *S.* Typhimurium SPI-1 T3SS is required to prevent the recruitment of Rab29 to the bacteria-containing vacuole. (*A*) Effect of coinfection with *S.* Typhimurium^{GFP} on the recruitment of CFP-Rab29 (green) to vacuoles containing *S.* Typhi^{mCherry} (red). (*B*) Effect of preinfection of cells with *S.* Typhimurium or *S.* Typhi on the recruitment of CFP-Rab29 (green) to vacuoles containing *S.* Typhi or *S.* Typhimurium^{mCherry} (red) 2 h after reinfection. Cells were preinfected with the strains indicated and reinfected 4 h later with *S.* Typhi or *S.* Typhimurium^{mCherry} (as indicated within the images). (*C* and *D*) Effect of mutations on the SPI-1 TTSS (Δ*invA* p*invasin*) or the SPI-2 TTSS (Δ*spiA*) or removal of all known effectors of the SPI-1 TTSS (Δeffectors p*invasin*) on the ability of *S.* Typhimurium to prevent the recruitment of CFP-Rab29 (green) to its vacuole. All strains expressed the fluorescent protein mCherry (red). (*E* and *F*) Ability of a *S.* Typhimurium mutant strain lacking all known effectors of the SPI-1 TTSS (Δeffectors) to prevent the recruitment of CFP-Rab29 (green) to the *S.* Typhi vacuole. Cells were infected with *S.* Typhi^{mCherry} (red) and reinfected with the strains indicated. *A*, *B*, *C*, and *E* show maximum-intensity projections of confocal Z-stacks. (Scale bars, 10 μm.) *D* and *F* show the mean ± SEM of the quantification of three independent experiments in which at least 100 bacteria were counted in each condition. Paired Student's *t* test analysis was performed and *P* values are shown. ***$P < 0.001$; **$P < 0.01$; *$P < 0.05$.

coinfected cultured cells expressing CFP-Rab29 with *S.* Typhi expressing the fluorescent protein mCherry (*S.* Typhi^{mCherry}), and *S.* Typhimurium expressing the fluorescent protein GFP and examined the ability of *S.* Typhi to recruit Rab29. We found that, in contrast to controls (i.e., cells infected just with *S.* Typhi), most of the *S.* Typhi^{mCherry}-containing vacuoles in cells coinfected with *S.* Typhimurium lacked Rab29 (Fig. 3*A*). In addition, we found that in cells preinfected with *S.* Typhimurium and reinfected 4 h after the first infection with *S.* Typhi^{mCherry}, very few *S.* Typhi^{mcherry}-containing vacuoles were decorated with Rab29 (5.4%) (Fig. 3*B*). In contrast, we found a much higher percentage (49.4%) of the *S.* Typhi^{mcherry}-containing vacuoles with Rab29 in cells preinfected with *S.* Typhi. *S.* Typhimurium^{mcherry} was not able to recruit Rab29 in cells preinfected with either *S.* Typhi or *S.* Typhimurium (Fig. 3*B*). These results indicate that a *S.* Typhimurium factor(s) acting in *trans* can prevent the localization of Rab29 to the bacteria-containing vacuole.

We investigated whether the factor(s) preventing Rab29 localization to the *S.* Typhimurium vacuole was an effector of one of its two T3SSs. As in wild type, we found that the *S.* Typhimurium Δ*spiA* mutant (defective in its SPI-2 T3SS) did not recruit Rab29 (Fig. 3 *C* and *D*), indicating that the factor(s) that prevents the localization of this GTPase to the bacteria-containing vacuole is not an effector of the SPI-2 T3SS. However, the *S.* Typhimurium Δ*invA* mutant (defective in the SPI-1 T3SS) internalized by Invasin effectively recruited Rab29 to its vacuole (Fig. 3 *C* and *D*). This result indicates that an effector(s) delivered through the SPI-1 T3SS is responsible for preventing Rab29 localization to the wild-type *S.* Typhimurium vacuole. To identify this effector(s) we first used a *S.* Typhimurium strain lacking all known SPI-1 T3SS effector proteins (i.e., Δ*sopE*, Δ*sopE2*, Δ*sopB*, Δ*sptP*, Δ*sopA*, Δ*sipA*, Δ*avrA*, Δ*sopD*, Δ*sopD2*, and Δ*slrP*). This strain is noninvasive because it lacks the effector proteins that mediate bacterial entry (i.e., SopE, SopE2, and SopB) (16). However, unlike the Δ*invA* mutant, the effectorless mutant strain is type III secretion and translocation competent (17). Surprisingly, when internalized via the Invasin protein, the *S.* Typhimurium effectorless mutant strain did not recruit Rab29 to its vacuole (Fig. 3 *C* and *D*). In addition, the *S.* Typhimurium effectorless strain without the Invasin plasmid,

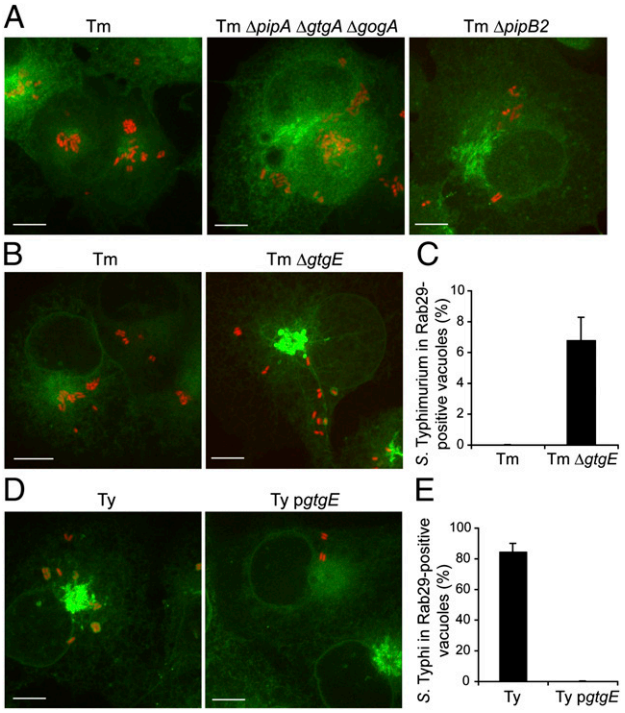

Fig. 4. GtgE, an effector of the *S.* Typhimurium SPI-1 T3SS, prevents the recruitment of Rab29 to the bacteria-containing vacuole. (*A*) COS-1 expressing CFP-Rab29 (green) were infected with *S.* Typhimurium^{mCherry} (Tm) and the indicated *S.* Typhimurium^{mCherry} isogenic mutant strains (red) and 3 h after infection the infected cells were visualized by fluorescence microscopy. Images show maximum-intensity projections of confocal Z-stacks. (Scale bars, 10 μm.) (*B–E*) COS-1 expressing CFP-Rab29 (green) were alternatively infected with *S.* Typhimurium^{mCherry} (Tm), its isogenic Δ*gtgE* mutant (Tm Δ*gtgE*), *S.* Typhi^{mCherry} (Ty), or the same strain expressing plasmid-borne *gtgE* (Ty p*gtgE*) (red), and 3 h after infection, infected cells were visualized by fluorescence microscopy. *B* and *D* show maximum-intensity projections of confocal Z-stacks. (Scale bars, 10 μm.) *E* and *F* show the mean ± SEM of the quantification of three independent experiments in which at least 100 bacteria were counted in each condition.

and therefore noninvasive but still able to attach to target cells and translocate effectors, was able to inhibit the recruitment of Rab29 to the *S.* Typhi^{mCherry} vacuole (Fig. 3 *E* and *F*). These results indicated that the activity of a yet unidentified SPI-1 T3SS effector(s) inhibits the recruitment of Rab29 to the *S.* Typhimurium-containing vacuole and that this putative effector can exert its function even when delivered by extracellularly localized bacteria.

To identify this effector, we examined by liquid chromatography (LC)-MS/MS the culture supernatants of a strain lacking all known SPI-1 T3SS effectors for the presence of previously unidentified putative SPI-1 T3SS effector proteins. This analysis detected the presence of the needle complex inner rod protein PrgJ (18); the needle complex assembly regulatory protein InvJ (19); and the T3SS effectors PipA, GogA, GtgA (20), and PipB2 (21) (*SI Appendix*, Fig. S9). However, deletion of the genes encoding these effectors did not result in the presence of Rab29 in the *S.* Typhimurium-containing vacuole (Fig. 4*A*). Our LC-MS/MS analysis also detected GtgE (22) (*SI Appendix*, Fig. S9), which is encoded on the Gifsy-2 bacteriophage of *S.* Typhimurium and other broad-host range serovars (23, 24), but, intriguingly, it is absent from the human-adapted *S.* Typhi and *S.* Paratyphi serovars. Although GtgE has not been demonstrated to be a T3SS effector protein, a bioinformatics tool (25) predicts the presence of a putative T3SS signal at its amino terminus. Consistent with this observation, we found that GtgE is secreted to culture supernatants in a SPI-1 T3SS-dependent manner (*SI Appendix*, Fig. S10). We therefore examined its potential involvement in the prevention of Rab29 recruitment to the *S.* Typhimurium vacuole. We found that a Δ*gtgE S.* Typhimurium mutant strain recruited Rab29 to its vacuole (Fig. 4 *B* and *C*). Furthermore, expression of *gtgE* in *S.* Typhi prevented recruitment of Rab29 to its vacuole (Fig. 4 *D* and *E*). These results indicate that GtgE is the SPI-1 T3SS effector protein whose activity prevents the recruitment of Rab29 to the *Salmonella*-containing vacuole.

GtgE is a protease that directly cleaves Rab29. During these studies we observed that, in comparison with cells infected with *S.* Typhi, the overall strength of the fluorescent signal of CFP-Rab29 was markedly reduced in cells infected with *S.* Typhimurium (Fig. 5*A*). In contrast, the reduction in CFP-Rab29 fluorescence was not observed in cells infected with the Δ*gtgE S.* Typhimurium mutant (Fig. 5*A*). We therefore examined the levels of Rab29 in cells infected with either *S.* Typhi or *S.* Typhimurium. We found that the levels of full-length Rab29 were markedly reduced in *S.* Typhimurium-infected cells compared with its levels in uninfected or *S.* Typhi-infected cells (Fig. 5*B*). Furthermore, a smaller molecular weight fragment of CFP-Rab29, presumably the result of its proteolytic cleavage, was detected in *S.* Typhimurium-infected cells but not in *S.* Typhi-infected or control uninfected cells (Fig. 5*B*). Cleavage of Rab29 in *S.* Typhimurium-infected cells was not prevented by the addition of a proteasome inhibitor (*SI Appendix*,

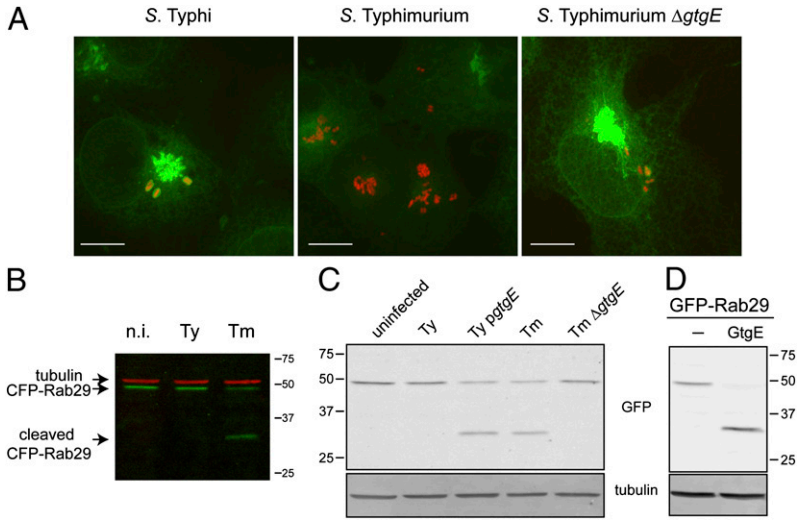

Fig. 5. Lack of Rab29 recruitment to the *S.* Typhimurium vacuole is due to its GtgE-dependent cleavage. (*A*) COS-1 cells expressing CFP-Rab29 (green) were infected with the indicated strains expressing the fluorescent protein mCherry (red) for 1 h, treated with 100 μg/mL gentamicin for 1 h, and imaged at 3 h postinfection. Images are maximum-intensity projections of confocal Z-stacks. In all cases, identical acquisition parameters were used to compare fluorescence intensity. (Scale bars, 10 μm.) (*B*) COS-1 cells expressing CFP-Rab29 were infected with *S.* Typhi or *S.* Typhimurium or left uninfected (n.i.) and 2.5-h cell lysates were analyzed by Western blotting using a rabbit anti-GFP antibody (green) and a mouse anti-tubulin antibody (red). (*C*) COS-1 cells expressing CFP-Rab29 were left uninfected or infected with *S.* Typhimurium (Ty), *S.* Typhimurium expressing plasmid-borne GtgE (Ty p*gtgE*), *S.* Typhimurium (Tm), or *S.* Typhimurium Δ*gtgE* (Tm Δ*gtgE*) and 2.5 h after infection they were analyzed by Western blotting using rabbit anti-GFP and mouse anti-tubulin antibodies. (*D*) COS-1 cells were cotransfected with a plasmid expressing GFP-Rab29 and a plasmid expressing GtgE or the vector control (–) and analyzed by Western blotting using rabbit anti-GFP and mouse anti-tubulin (as loading control) antibodies.

Fig. S11), suggesting that this protein degradation pathway is not involved in this process. To investigate the potential role of GtgE in Rab29 cleavage, we infected cells with the *S.* Typhimurium Δ*gtgE* mutant or with *S.* Typhimurium expressing plasmid-borne GtgE and examined the levels of Rab29 in lysates of infected cells. We found that Rab29 was not cleaved in cells infected with *S.* Typhimurium Δ*gtgE* but was cleaved in cells infected with *S.* Typhimurium expressing *gtgE* (Fig. 5*C*). To test the potential specificity of the GtgE activity, we examined the effect of *S.* Typhimurium infection on the stability of the related GTPases, Rab40B, Rab5, and Rab7. We found that *S.* Typhimurium infection did not result in the degradation of any of these related GTPases (*SI Appendix*, Fig. S12), suggesting a narrow specificity in the activity of GtgE. To investigate whether GtgE by itself could mediate the cleavage of Rab29, we coexpressed GtgE and Rab29 and examined the levels of Rab29 by fluorescence and Western blot analysis. We found a drastic reduction of the fluorescence of CFP-Rab29 in cells expressing GtgE (*SI Appendix*, Fig. S13). In addition, in cell lysates of cotransfected cells, we found a GFP-Rab29 cleavage pattern similar to that observed in wild-type *S.* Typhimurium-infected cells (Fig. 5*D*). Taken together these results indicate that GtgE mediates the cleavage of Rab29 and that no other bacterial factor is required for this activity. Furthermore our results indicate that the GtgE activity is rather restricted because it is not directed to other highly related GTPases.

To gain insight into the potential mechanism of action of GtgE, we examined its primary amino acid sequence. We identified significant similarities to cysteine proteinases of the papain subfamily (*SI Appendix*, Fig. S14) as well as potential key conserved catalytic residues in GtgE (e.g., His151) (*SI Appendix*, Fig. S14). Introduction of a mutation in this predicted catalytic residue completely abolished the ability of GtgE to mediate Rab29 cleavage (Fig. 6*A*). Coexpression in *Escherichia coli* of wild-type GtgE with Rab29 resulted in the cleavage of the GTPase although coexpression of the catalytic mutant GtgE^{H151A} did not (Fig. 6 *B* and *C*). Furthermore, purified GtgE was able to cleave purified Rab29 (Fig. 6*D*), and cleavage required the presence of divalent cations (*SI Appendix*, Fig. S15). These results indicate that GtgE is a protease that directly targets Rab29 for cleavage. We investigated the site of GtgE cleavage by determining the amino-terminal sequence of the Rab29 C-terminal cleavage product. We found that GtgE cleaves between glycine 41 and valine 42 of Rab29 (Fig. 6 *E* and *F*). The cleavage site is located between a critical loop and strand of the predicted structure of Rab29 (Fig. 6*E*), and it is expected to fully inactivate this GTPase because the cleavage product lacks the GTPase putative switch 1 region and part of its putative Rab complementarity-determining region (RabCDR), which is required for the interaction of Rab GTPases with their effectors (Fig. 6*F*) (26, 27).

GtgE influences the ability of *Salmonella* to replicate within macrophages. Previous studies have shown that GtgE is required for *S.* Typhimurium virulence in an animal model of infection (22). This observation prompted us to investigate the potential influence of the presence of this effector in the ability of *S.* Typhi to replicate within macrophages. We found that the *S.* Typhi strain encoding wild-type GtgE replicated significantly better that the strains encoding the mutant effector (Fig. 6*G*). These results are consistent with the hypothesis that the removal of Rab29 from the *Salmonella*-containing vacuole results in an environment that is more favorable for *Salmonella* growth. Furthermore, consistent with the involvement of Rab29 in typhoid toxin transport, *S.* Typhi expressing wild-type GtgE exhibited decreased efficiency in the formation of the typhoid toxin transport intermediates (*SI Appendix*, Fig. S16).

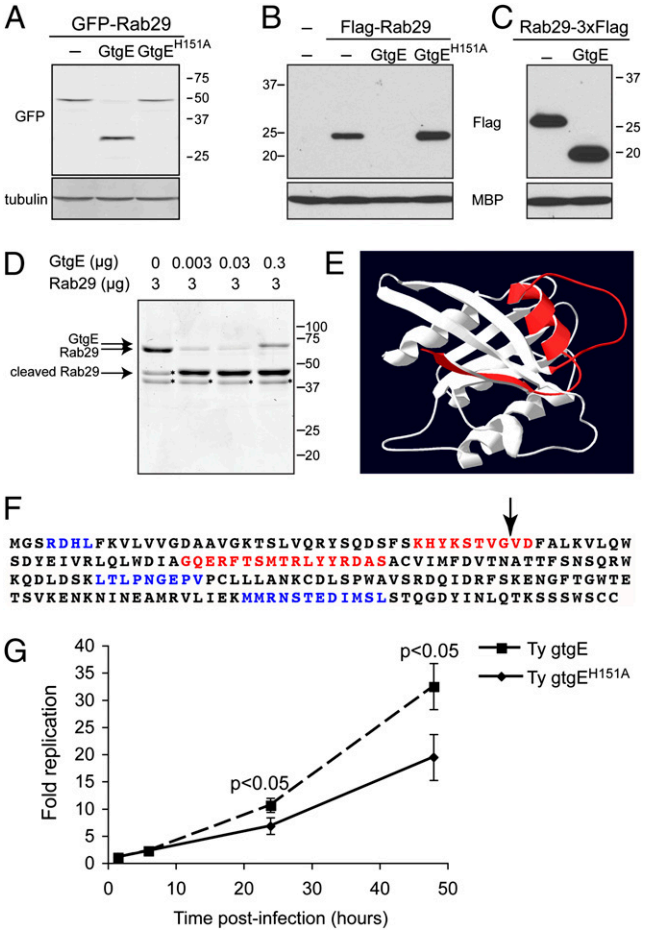

Fig. 6. GtgE is a protease that directly targets Rab29. (*A*) COS-1 cells were cotransfected with a plasmid expressing GFP-Rab29 and a plasmid expressing GtgE, GtgE^{H151A}, or the vector control (–) and analyzed by Western blotting using rabbit anti-GFP and mouse anti-tubulin (as loading control) antibodies. (*B* and *C*) *E. coli* DH5a was transformed with a plasmid expressing amino- (*B*) or carboxy- (*C*) terminally FLAG-tagged Rab29 or the empty vector (–), along with a compatible plasmid expressing GtgE, the catalytic mutant GtgE^{H151A}, or the empty vector (–), as indicated. Bacterial lysates were analyzed by Western blotting using anti-Flag and anti-*E. coli* maltose-binding protein (MBP) (as loading control) antibodies. (*D*) Indicated amounts of purified MBP-tagged Rab29 and MBP-tagged GtgE were incubated at 37 °C for 30 min in the presence of 10 mM $CaCl_2$ and $MgCl_2$. Proteins were separated by SDS/PAGE and stained with Coomassie. Asterisks indicate protein bands that were already present in the purified Rab29 material that are not the result of GtgE activity. (*E*) The Rab29 atomic structure was modeled using the Swissmodel server (http://swissmodel.expasy.org/) and visualized using the DeepView Swiss Pdb viewer. The amino-terminal segment of Rab29, which is removed by GtgE cleavage, is highlighted in red. (*F*) Rab29 amino acid sequence indicating the GtgE cleavage site (arrow) and the location of the putative switch I and switch II regions (red) and the putative Rab complementarity-determining region (blue). (*G*) THP-1 human macrophage cells were infected with *S.* Typhi expressing plasmid-borne GtgE or the catalytic inactive mutant GtgE^{H151A}. Cells were lysed at the indicated time points and colony-forming units enumerated. Values are means ± SEM of fold increase at each time point over the values at 1.5 h postinfection from three independent experiments. *P* values were determined by Student's *t* test.

Discussion

The molecular bases for the different pathogenic properties of human-adapted and broad-host *Salmonellae* are presently unknown. A screen to identify host factors required for the export of typhoid toxin, which is exclusively encoded by the human-specific *S. enterica* serovars *S.* Typhi and *S.* Paratyphi, identified Rab40B and Rab29. Although the localization of Rab40B did not

change upon bacterial infection, we found that Rab29 was effectively recruited to the *S.* Typhi and *S*. Paratyphi-containing vacuoles. However, we found that Rab29 was not recruited to vacuoles containing broad-host range *S. enterica* serovars such as *S.* Typhimurium and *S*. Enteritidis. We also found that the absence of Rab29 from the vacuole of broad-host *Salmonellae* is due to its specific cleavage by GtgE, a type III secreted effector protein absent from the human-adapted *S*. Typhi and *S.* Paratyphi serovars. The protease activity of GtgE appears to have rather narrow target specificity because it did not cleave the related GTPases Rab40B, Rab5, and Rab7. In this regard, the narrow specificity of a bacterially encoded protease is reminiscent of other bacterially encoded virulence factors such as tetanus and botulinum toxins, which target specific components of the synaptic vesicle (28). Although nothing is known about the biology of Rab29, it is expected that the presence or absence of this GTPase on *Salmonella*-containing vacuoles should significantly change the properties of these compartments given the role that Rab-family GTPases in general are known to play in regulating vesicle trafficking. Our intriguing observation that Rab29 localizes to dynamic areas of the Golgi apparatus and within tubes emanating from the *S*. Typhi-containing vacuole toward the cell periphery suggests the potential involvement of these structures in typhoid toxin transport. However, given the lack of knowledge on the biology of Rab29, more experiments will be required to clarify the specific role of this GTPase in toxin transport.

It is not clear how the specific targeting of Rab29 benefits *Salmonella* pathogenesis. Because deletion of *gtgE* results in a very significant virulence reduction in a mouse model of infection (22), removal of Rab29 from infected cells should be advantageous for the pathogenesis of *S.* Typhimurium. However, although GtgE appears to have narrow substrate specificity, it is possible that GtgE may target other Rab GTPases so additional experiments on the specificity of this protease will be required to clarify its role in virulence. Interestingly, expression of GtgE in *S*. Typhi resulted in increased growth within cultured macrophages (although not within epithelial cells), indicating that the activity of this effector favors intracellular growth. Unlike *S*. Typhimurium a critical feature of *S*. Typhi is its ability to cause persistent infection. It is therefore possible that slowing down intracellular growth by recruiting Rab29 may be beneficial for the establishment of persistent infection because slower replication may be necessary to avoid immune detection.

Overall this study revealed significant differences between the intracellular compartments of human-adapted and broad-host *S. enterica* serovars, which may have implications for the understanding of the rather marked differences between the biology of these different *Salmonella* serovars. In addition, our results indicate a remarkable fine-tuning of the activity of T3SSs to adapt their function to the unique requirements of each *S. enterica* serovar because differences in a single type III secretion effector protein result in fundamental changes in *Salmonella*'s intracellular niche.

Materials and Methods

Detailed information about experimental procedures and strains can be found in *SI Appendix, Materials and Methods*. Wild-type *S. enterica* strains have been described previously (29, 30). Mutants were constructed and bacterial infections were carried out as previously described (31). Live-cell imaging was performed at 37 °C in a temperature, humidity, and CO_2 controlled live chamber (Pathology Devices), using a 60× oil objective (numerical aperture, 1.4) of an Improvision spinning disk confocal microscope equipped with a Nikon TE2000. The FLAG fluorescence associated with puncta (not associated with bacteria) was quantified by using a purpose-built macro developed in the open source software ImageJ (http://rsbweb.nih.gov/ij/). Mass spectrometry analysis was carried out as previously described (32).

ACKNOWLEDGMENTS. We thank members of the J.E.G. laboratory for careful review of this manuscript. We also thank Massimiliano Baldassarre for help in writing the ImageJ macro for image quantification. This work was supported by National Institute of Allergy and Infectious Diseases Grants AI079022, AI070949, and AI055472 (to J.E.G.).

1. Pang T, Levine MM, Ivanoff B, Wain J, Finlay BB (1998) Typhoid fever—important issues still remain. *Trends Microbiol* 6:131–133.
2. Crump JA, Mintz ED (2010) Global trends in typhoid and paratyphoid fever. *Clin Infect Dis* 50:241–246.
3. Parry CM, Hien TT, Dougan G, White NJ, Farrar JJ (2002) Typhoid fever. *N Engl J Med* 347:1770–1782.
4. Hohmann EL (2001) Nontyphoidal salmonellosis. *Clin Infect Dis* 32:263–269.
5. Sabbagh SC, Forest CG, Lepage C, Leclerc JM, Daigle F (2010) So similar, yet so different: Uncovering distinctive features in the genomes of Salmonella enterica serovars Typhimurium and Typhi. *FEMS Microbiol Lett* 305:1–13.
6. Spanò S, Ugalde JE, Galán JE (2008) Delivery of a Salmonella Typhi exotoxin from a host intracellular compartment. *Cell Host Microbe* 3:30–38.
7. Haghjoo E, Galán JE (2004) Salmonella typhi encodes a functional cytolethal distending toxin that is delivered into host cells by a bacterial-internalization pathway. *Proc Natl Acad Sci USA* 101:4614–4619.
8. Song J, et al. (2010) A mouse model for the human pathogen Salmonella typhi. *Cell Host Microbe* 8:369–376.
9. Brighouse A, Dacks JB, Field MC (2010) Rab protein evolution and the history of the eukaryotic endomembrane system. *Cell Mol Life Sci* 67:3449–3465.
10. Stenmark H (2009) Rab GTPases as coordinators of vesicle traffic. *Nat Rev Mol Cell Biol* 10:513–525.
11. Méresse S, Steele-Mortimer O, Finlay BB, Gorvel JP (1999) The rab7 GTPase controls the maturation of Salmonella typhimurium-containing vacuoles in HeLa cells. *EMBO J* 18:4394–4403.
12. Wasmeier C, et al. (2006) Rab38 and Rab32 control post-Golgi trafficking of melanogenic enzymes. *J Cell Biol* 175:271–281.
13. Galán JE (2001) Salmonella interactions with host cells: Type III secretion at work. *Annu Rev Cell Dev Biol* 17:53–86.
14. Waterman SR, Holden DW (2003) Functions and effectors of the Salmonella pathogenicity island 2 type III secretion system. *Cell Microbiol* 5:501–511.
15. Ibarra JA, Steele-Mortimer O (2009) Salmonella—the ultimate insider. Salmonella virulence factors that modulate intracellular survival. *Cell Microbiol* 11:1579–1586.
16. Zhou D, Chen LM, Hernandez L, Shears SB, Galán JE (2001) A Salmonella inositol polyphosphatase acts in conjunction with other bacterial effectors to promote host cell actin cytoskeleton rearrangements and bacterial internalization. *Mol Microbiol* 39:248–259.
17. Hernandez LD, Pypaert M, Flavell RA, Galán JE (2003) A Salmonella protein causes macrophage cell death by inducing autophagy. *J Cell Biol* 163:1123–1131.
18. Marlovits TC, et al. (2006) Assembly of the inner rod determines needle length in the type III secretion injectisome. *Nature* 441:637–640.
19. Kubori T, Sukhan A, Aizawa SI, Galán JE (2000) Molecular characterization and assembly of the needle complex of the Salmonella typhimurium type III protein secretion system. *Proc Natl Acad Sci USA* 97:10225–10230.
20. Wood MW, et al. (1998) Identification of a pathogenicity island required for Salmonella enteropathogenicity. *Mol Microbiol* 29:883–891.
21. Knodler LA, et al. (2003) Salmonella type III effectors PipB and PipB2 are targeted to detergent-resistant microdomains on internal host cell membranes. *Mol Microbiol* 49:685–704.
22. Ho TD, et al. (2002) Identification of GtgE, a novel virulence factor encoded on the Gifsy-2 bacteriophage of Salmonella enterica serovar Typhimurium. *J Bacteriol* 184:5234–5239.
23. McClelland M, et al. (2004) Comparison of genome degradation in Paratyphi A and Typhi, human-restricted serovars of Salmonella enterica that cause typhoid. *Nat Genet* 36:1268–1274.
24. Parkhill J, et al. (2001) Complete genome sequence of a multiple drug resistant Salmonella enterica serovar Typhi CT18. *Nature* 413:848–852.
25. Buchko GW, et al. (2010) A multi-pronged search for a common structural motif in the secretion signal of Salmonella enterica serovar Typhimurium type III effector proteins. *Mol Biosyst* 6:2448–2458.
26. Ostermeier C, Brunger AT (1999) Structural basis of Rab effector specificity: crystal structure of the small G protein Rab3A complexed with the effector domain of rabphilin-3A. *Cell* 96:363–374.
27. Lee MT, Mishra A, Lambright DG (2009) Structural mechanisms for regulation of membrane traffic by rab GTPases. *Traffic* 10:1377–1389.
28. Montecucco C, Schiavo G (1993) Tetanus and botulism neurotoxins: A new group of zinc proteases. *Trends Biochem Sci* 18:324–327.
29. Galán JE, Curtiss R, 3rd (1991) Distribution of the invA, -B, -C, and -D genes of Salmonella typhimurium among other Salmonella serovars: invA mutants of Salmonella typhi are deficient for entry into mammalian cells. *Infect Immun* 59:2901–2908.
30. Hoiseth SK, Stocker BA (1981) Aromatic-dependent *Salmonella typhimurium* are nonvirulent and effective as live vaccines. *Nature* 291:238–239.
31. Kaniga K, Bossio JC, Galán JE (1994) The Salmonella typhimurium invasion genes invF and invG encode homologues of the AraC and PulD family of proteins. *Mol Microbiol* 13:555–568.
32. Lara-Tejero M, Kato J, Wagner S, Liu X, Galán JE (2011) A sorting platform determines the order of protein secretion in bacterial type III systems. *Science* 331:1188–1191.